POLITECNICO DI TORINO
Repository ISTITUZIONALE

Stabilising CDW recycled aggregates with alternatives to Portland cement

Original
Stabilising CDW recycled aggregates with alternatives to Portland cement / Tefa, L., Bianco, I., Bassani, M.. - In: CONSTRUCTION AND BUILDING MATERIALS. - ISSN 0950-0618. - 471:(2025). [10.1016/j.conbuildmat.2025.140705]

Availability:
This version is available at: 11583/2998841 since: 2025-04-04T07:47:15Z

Publisher:
Elsevier Ltd

Published
DOI:10.1016/j.conbuildmat.2025.140705

Terms of use:

This article is made available under terms and conditions as specified in the corresponding bibliographic description in the repository

Publisher copyright

(Article begins on next page)

19 November 2026

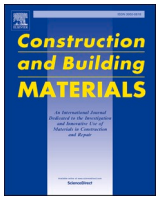
Construction and Building Materials 471 (2025) 140705



Contents lists available at ScienceDirect

Construction and Building Materials

journal homepage: www.elsevier.com/locate/conbuildmat





Stabilising CDW recycled aggregates with alternatives to Portland cement

Luca Tefa *, Isabella Bianco, Marco Bassani

Department of Environment, Land and Infrastructure Engineering, Politecnico di Torino, Italy

ARTICLE INFO

Keywords:
Construction and demolition waste aggregate
Stabilised granular materials
Alkali-activation
Pozzolanic cement
Mechanical properties
Life cycle assessment

ABSTRACT

The use of ordinary Portland cement for the stabilisation of granular materials in road construction undermines the effort on sustainability made by using recycled aggregate in substitution of natural ones. This requires the use of low-impact binders so that the road construction industry complies with the prevailing environmental regulations. This study compares the mechanical and environmental properties of construction and demolition waste (CDW) aggregates stabilised with different binders: (i) a Portland-limestone cement as a reference, (ii) a pozzolanic cement, (iii) an experimental pozzolanic cement containing waste clay from the lightweight aggregate production, and (iv) a binder with alkali-activated CDW fines. In the laboratory experiments, both strength and resilient properties were considered, while the environmental impact was assessed in a cradle-to-gate scenario through a life cycle analysis (LCA). The stabilised mixture with pozzolanic cement achieved comparable strength and stiffness while exhibiting a lower environmental impact than the mixture containing Portland-limestone cement. The addition of waste clay to the pozzolanic cement significantly reduces its environmental impact albeit more binder is required to compensate for the lower mechanical properties. The alkaline activation of the fine particles in the CDW aggregate enabled the creation of a stabilised mixture with high strengths and resilient modulus. However, this alternative stabilisation technique requires further optimisation to mitigate the significant environmental impact. The engineering evaluations of the stabilised granular mixtures studied have considered both mechanical and environmental factors intending to contribute to the scientific debate on how to make roadworks sustainable and conserve natural resources.

1. Introduction

The use of construction and demolition waste (CDW) recycled aggregates (RA) in road construction is becoming widespread due to the promotion of circular economy policies [1,2] and their general availability worldwide [3,4]. Several laboratory and on-site experimental studies demonstrated the feasibility of using CDW-RA in substitution of (primary) natural aggregate for the formation of embankments and subgrade layers of roads [5–9]. Their use in pavement layers such as subbases and bases may necessitate cement stabilisation as is the case with natural aggregates [10–13]. However, the use of ordinary Portland cement (OPC) is unfavourable in sustainability terms as a lot of energy is expended in its production, resulting in the emission of significant quantities of carbon dioxide (CO_2), which is a substantial contributor to climate change.

The construction industry is exploring the use of alternative binders such as low-carbon blended cements [14–16]. Conversely, alkali-activated (AA) binders are gaining interest thanks to their performance and their potentially lower environmental impact in comparison to OPC. Some life cycle assessment (LCA) studies have indicated that AA binders with fly ash (FA) and metallurgical slag (e.g., blast furnace slag) result in a reduction in greenhouse gas emissions of between 30 % and 80 % in comparison to OPC [17–19]. However, those estimates vary widely and remain a subject of debate, mostly because of the high impact of the chemical alkaline activators used to trigger the AA process [20,21]. Metakaolin, FA, and blast furnace slag (BFS) are the most common precursors for the AA process [22,23]. Natural pozzolans, ferrous or non-ferrous slags, Ca-rich materials, and other by-products and waste sources have also been exploited [24–30].

In a previous study [31], we observed that the addition of

Abbreviations: AA, Alkali-activated; AS, Alkaline solution; AS_{opt}, Optimum alkaline solution content; BFS, Blast furnace slag; CDW, Construction and demolition waste; FA, fly ash; IP, Industrial pozzolana; ITS, Indirect tensile strength; LCA, Life-cycle assessment; LOI, Loss of ignition; M-EPDG, Mechanistic-empirical pavement design guide; OPC, Ordinary Portland cement; RA, Recycled aggregates; RM, Resilient modulus; UCS, Unconfined compressive strength; WC, Waste clay; w_{opt}, Optimum water content; XRF, X-ray fluorescence; $\gamma_{d,max}$, Maximum dry density.

* Corresponding author.
E-mail addresses: luca.tefa@polito.it (L. Tefa), isabella.bianco@polito.it (I. Bianco), marco.bassani@polito.it (M. Bassani).

https://doi.org/10.1016/j.conbuildmat.2025.140705
Received 12 December 2024; Received in revised form 14 February 2025; Accepted 3 March 2025
Available online 8 March 2025
0950-0618/© 2025 The Author(s). Published by Elsevier Ltd. This is an open access article under the CC BY-NC-ND license (http://creativecommons.org/licenses/by-nc-nd/4.0/).

Portland-limestone cement to stabilise CDW-RA mixtures significantly reduced the benefits of using CDW-RA in road pavement applications. Although a stiffer cement-stabilised subbase layer reduces the thickness of the bituminous layers by 2.0 cm compared to the solution with a subbase consisting of unbound CDW-RA, the inclusion of cement results in a climate change increment of +30 % when the entire road pavement structure is considered. A comparison of the environmental impact of the two materials reveals a dramatic advantage for the unbound CDW-RA, with the stabilised mixtures having a climate change impact which is approximately 350 % higher. Other studies have investigated the use of alternative binders to stabilise road subbases containing RA, demonstrating that acceptable mechanical performance can be achieved with cheaper binders [32–36]. However, many of these studies have not assessed the actual environmental impact of CDW-RA mixtures with different binders.

To the best of the authors' knowledge, there is a lack of comprehensive environmental and structural studies comparing different binders and promoting the most appropriate ones for optimising the structural and environmental performances of stabilised CDW-RA.

Therefore, in this study, we investigated and compared the mechanical properties and environmental performances of CDW aggregate stabilised with sustainable cementitious and AA binders, taking into account their local availability in Northwest Italy. The following binders were selected for potential stabilisation of CDW-RA: (i) a Portland-limestone cement (reference); (ii) a pozzolanic cement with industrial pozzolana (IP, i.e., siliceous fly ash from coal combustion); (iii) an experimental pozzolanic cement with waste clay (WC) from the production of expanded clay; and (iv) fines (< 0.063 mm) from the recovery of CDW material to be AA [37]. Due to their very low availability in Northwest Italy and their relatively high costs, FA and BFS precursors for AA were not investigated. The strength (compressive and indirect tensile strength) and stiffness (resilient modulus) of stabilised CDW-RA mixtures with different binders were measured and an LCA analysis was conducted to identify and quantify the environmental impacts associated with the production of these materials.

2. Materials

2.1. Binders

A CEM-II/B 32.5 R Portland-limestone cement and a CEM-IV/B (V) 32.5 N pozzolanic cement according to EN 197–1 [38] were employed together with an alternative binder obtained by mixing 50 % by mass of CEM-IV/B and 50 % by mass of WC, designated as CEM-IV/H ("hybrid" type IV cement).

The chemical composition as determined by X-ray fluorescence (XRF) is given in Table 1. CEM-II/B is predominantly composed of calcium and silicon oxides (CaO) in line with the literature [39,40]. The chemical composition of CEM-IV/B and CEM-IV/H is influenced by the presence of the IP and WC, respectively. In these cases, the CaO content is reduced in favour of a considerable increase in SiO_2 and Al_2O_3.

Table 1
XRF of cement powders and precursors of AA binders.

Constituent	Content (%)			
	CEM-II/B	CEM-IV/B	CEM-IV/H	CDW fines
CaO	69.15	41.90	22.85	12.00
SiO_2	12.75	30.00	43.60	52.30
Al_2O_3	3.10	9.24	14.47	16.10
MgO	1.16	2.31	3.05	5.53
Na_2O	2.59	2.25	1.82	1.24
SO_3	4.99	4.70	2.67	1.59
Cl	0.33	0.25	0.17	0.10
K_2O	1.53	2.93	3.46	2.80
Fe_2O_3	2.50	4.89	6.49	6.37
TiO_2	0.19	0.43	0.58	0.66
LOI	1.16	0.56	0.30	0.66

Preliminary X-ray diffraction analyses of WC indicate a highly crystalline powder, with quartz showing the highest intensity of the phases detected. In addition, aluminosilicate phases such as ringwoodite (magnesium iron silicate) and albite (sodium aluminium silicate) have also been detected.

To activate the alkaline reaction in the CDW-RA mixture, an aqueous sodium silicate solution (Na_2SiO_3) was used. This alkaline solution (AS) had a SiO_2/Na_2O mass ratio of 1.65 (SiO_2 = 22.2 %, Na_2O = 13.4 %, H_2O = 64.4 %) and a density of 1.43 g/ml at 20°C. Previous studies have shown that fines from CDW materials can be alkali-activated without thermal treatment [28]. In fact, the addition of AS to CDW-RA containing fine particles helps to form a binder without highly reactive aluminosilicate fines, e.g., FA or BFS [41].

Apart from the slightly higher SiO_2 content, the chemical composition of the CDW fines (Table 1) was consistent with previous investigations [28,37]. The lower loss of ignition (LOI) value compared to previous studies is attributed to the presence of silicate-based minerals in the CDW fines with crystalline phases of quartz, silicate and sulphate groups including albite, gedrite, muscovite, clinochlore, and thaumasite. Preliminary X-ray diffraction analysis of the CDW fines also confirms the presence of calcium carbonate.

2.2. Aggregates

The CDW aggregate in the 0–40 mm size fraction was collected from a recycling plant in the Turin area (Northwest of Italy) according to EN 932–1 [42] and then sieved to 25 mm for preparing specimens. In this plant, waste (CDW) and natural soils and rocks are screened, cleaned, crushed, and sieved to produce unselected CDW-RA containing particles of crushed concrete, reclaimed bituminous mixtures, ceramics (bricks and tiles), and natural aggregates. The percentage of each constituent was evaluated according to EN 933–11 [43] and the results are shown in Fig. 1-a. This CDW composition is representative of unselected CDW collected from a mixed waste stream with the predominance of concrete and natural materials [44,45]. Furthermore, Fig. 1-b illustrates the particle size distribution of the sampled CDW material (sieved at 25 mm) compared to the Italian Technical Specifications [46].

The particle's density of CDW-RA was found to be 2597 kg/m^3 with water absorption of 3.7 % (EN 1097–6; [47]). The CDW-RA exhibited a flakiness index of 12 % and a shape index of 14 % evaluated according to EN 933–3 [48] and EN 933–4 [49], respectively.

3. Methods

3.1. Experimental flow, specimen preparation, and mechanical testing

The experimental investigation was divided into two parts: (i) a preliminary selection of the binder content (part 1) and (ii) a comparative analysis of the different binders (part 2), as shown in Fig. 2. In part 1, the CDW-RA was stabilised with three dosages of CEM-II/B to establish the reference binder content, by varying it between 2, 3, and 4 % of the dry aggregate mass. In part 2, the same amount (i.e., 3 %) of the cementitious binders was added to the CDW-RA mixtures. A Proctor test was also carried out to determine the optimum water (w_{opt}) and alkaline solution (AS_{opt}) contents to achieve the maximum dry density ($\gamma_{d,max}$), according to the modified procedure of EN 13286–2 [50].

Cylindrical specimens for mechanical testing were prepared by manually mixing the aggregate, binder, and liquid phase (water or AS), and then compacted in the gyratory shear compactor to achieve the target Proctor density (Fig. 2). A constant vertical pressure of 600 kPa was applied in the compactor with shear stresses induced by the gyration and the 1.25° tilt angle of the mould. The rotation speed was set at 30 rpm, while the maximum number of gyrations was set at 100 to limit the excessive degradation of weaker particles (e.g., bricks) contained in the CDW material [44]. Specimens measuring 100 × 200 mm (diameter × height) were compacted in four layers of equal thickness to determine

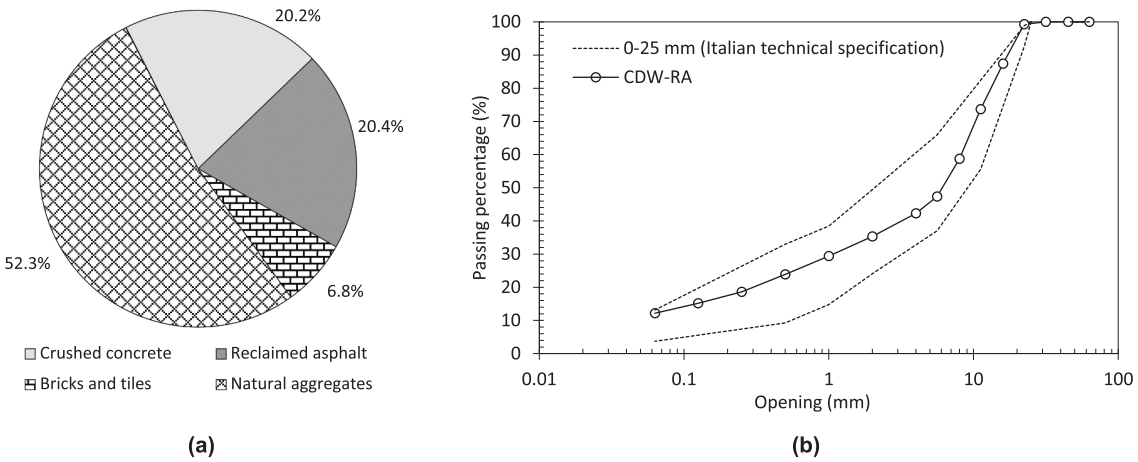


Fig. 1. (a) Percentage of constituent included in CDW-RA. (b) Particle size distribution.

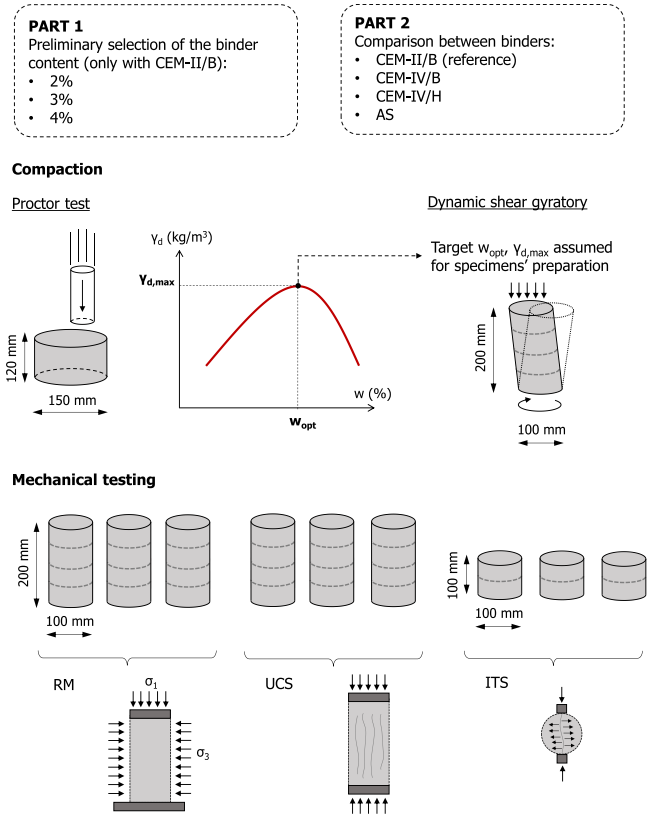


Fig. 2. Experimental flow (RM = resilient modulus, UCS = unconfined compression strength, ITS = indirect tensile strength).

the resilient modulus (RM) and unconfined compressive strength (UCS), while specimens measuring 100 × 100 mm (diameter × height) were used for indirect tensile strength (ITS) tests. After compaction, specimens were extracted from the metallic compactor moulds and placed in plastic moulds to prevent any damage during handling. Specimens were cured at room temperature (20 °C) and relative humidity higher than 90 % for 7 days. Three replicates of the same mixtures were made to ensure statistical representativeness (Fig. 2).

Repeated load triaxial tests to estimate the RM were carried out according to the AASHTO T307 base/subbase protocol [51] in a triaxial machine with two displacement transducers placed outside the cell. The results were modelled according to the Mechanistic-Empirical Pavement Design Guide (M-EPDG) to assess the evolution of RM as a function of the stress state. In the M-EPDG model of Eq. 1, θ is the first invariant (i.e., the sum of the three principal stresses during the test $\theta = \sigma_1 + \sigma_2 + \sigma_3$), τ_{oct} is the octahedral shear stress (i.e., $\sqrt{3}/2 \cdot (\sigma_1 - \sigma_3)$, and p_a is the reference atmospheric pressure [52]:

$$RM = k_1 \cdot p_a \cdot \left(\frac{\theta}{p_a}\right)^{k_2} \cdot \left(1 + \frac{\tau_{oct}}{p_a}\right)^{k_3} \quad (1)$$

where k_1, k_2, and k_3 are the regression parameters depending on the material. The coefficient k_1 represents the model intercept (i.e., the value of RM when no other factors are contributing) and is proportional to Young's modulus [53]. The coefficient k_2 is associated with the first stress invariant and it is generally greater than 0 for unbound and stabilised granular materials. When $k_2 > 0$, the material exhibits a stress-stiffening behaviour, i.e., as the stress invariant increases, the stiffness of the material also increases [54]. Finally, k_3 is the regression coefficient associated with the octahedral shear stress, which measures the ability of the material to resist shear stress. If k_3 is positive, the material exhibits shear hardening, i.e. it becomes more resistant to deformation as the shear stress increases. Conversely, if k_3 is negative, the material exhibits a shear-softening attitude [55].

The UCS and ITS tests were carried out using a 50 kN compression machine, applying a constant displacement rate of 0.5 mm/min, in accordance with previous investigations [41].

3.2. Environmental assessment

The life cycle assessment (LCA) methodology is based on the ISO standards 14040–44 [56,57] and the latest available European Commission guidelines [58,59]. In this paper, the LCA analysis compares the environmental performance of stabilised CDW-RA that have similar mechanical properties and have been produced with different binder types. The boundaries of the study were "cradle-to-gate", covering the entire supply chain of the products, i.e., from the extraction of the raw materials to the production of the final stabilised mixture. The impact results are presented with the reference to 1 Mg of stabilised CDW-RA (functional unit) produced [60]. An attribution approach that does not consider the environmental benefits associated with avoided products was adopted. In particular, it does not take into account the environmental benefits of avoiding landfilling for CDW or substituting natural aggregates. The *Ecoinvent* 3.9.1 database was used as a source of background data [61]. The Environmental Footprint 3.1 method [62] was adopted to calculate the environmental impacts, and the results for all 16 available indicators were provided to facilitate comparison with other studies.

The inventory for the production of CDW-RA was derived from primary data collected in 2022 by a producer located in the Northwest of

Table 2
Life cycle inventory of 1 Mg of CDW-RA.

Flow	Quantity	Unit of measure	Note
Outputs			
CDW-RA	1.0	Mg	
Generic waste	3.2	kg	Untreated waste from the CDW recycling process
Inputs			
Fuel	5.8	MJ	Diesel burned in building machines
Electricity MV	1.42	MJ	MV = Medium voltage
Electricity LV	$3.31 \cdot 10^{-1}$	MJ	LV = Low voltage from photovoltaic
Lubricating oil	$2.24 \cdot 10^{-3}$	kg	
Water	2.24	l	
Transport of CDW	20	Mg·km	Transport of CDW from demolition site to recycling plant

Italy, with a total production of 382,359 Mg [63]. The activities of the recycling plant included (i) CDW collection, (ii) feeding and transport on belts, (iii) sorting and cleaning operations, (iv) crushing, (v) storage with trucks and conveyor belts, and (iv) disposal or treatment of other waste source material (i.e., paper, steel, hazardous waste). The process results in the production of CDW-RA with different grain size distributions. A comprehensive inventory of the recycled aggregates is given in Table 2. The inventory analysis for CEM-II/B and CEM-IV/B is given in Table 3. The data was obtained from companies located in the northern region of Italy, with 2022 as the reference year. Where necessary, this data was supplemented by the *Ecoinvent* 3.9.1 database [61]. The IP contained in the CEM-IV/B was a by-product of the heat generated by the coal-fired furnaces, while the WC added to the CEM-IV/B to form the CEM-IV/H was considered a by-product of the expanded clay production. In both cases, an economic allocation was used to calculate the impact of these two by-products. For the production of stabilised CDW-RA mixtures, a distance of 150 km from the cement plant to the mixing facility was assumed for CEM-II/B and CEM-IV/B. For WC, the distance was set at 300 km, while for AS, the transport distance was set at 250 km.

4. Results

4.1. Phase 1: selection of the binder content

Fig. 3 shows the results of the Proctor compaction test conducted on CDW-RA stabilised with CEM-II/B to select the optimum binder content (2, 3, or 4 %). Although all mixtures required 8.5 % of water to achieve the maximum densification, the highest value of $\gamma_{d,max}$, equal to 2119 kg/m^3, was obtained with 3 % of CEM-II/B.

The UCS and ITS results obtained from 7-day cured specimens are shown in Fig. 4-a. The average value of UCS increased from 1.45 to 1.97 MPa as the cement content increased from 2 % to 4 %. As expected, the higher cement content resulted in a greater hydration reaction activity and a greater resistance to external loading. It is worth noting that CDW-RA mixtures with 3 and 4 % of CEM-II/B comply with the lower limit of UCS = 1.72 MPa (250 psi) of cement stabilised mixture for subbase/subgrade layers for flexible pavements according to M-EPDG requirements [64,65].

The results for ITS mirror those for the UCS. The CEM-II/B stabilised mixtures experienced an increase in the average ITS from 0.209 to 0.294 MPa as the addition of cement increased from 2 % to 4 %. Similarly, CDW-RA materials containing 3 and 4 % of CEM-II/B showed an average ITS that exceeded the 0.250 MPa threshold established in the Italian Technical Specifications [46].

Fig. 4-b shows the evolution of the resilient modulus (RM) as a function of the first invariant (θ). It is worth noting that the choice of cement content affects the RM of the stabilised CDW-RA mixture. The mixture containing 3 % of CEM-II/B consistently exhibits the highest RM values across all investigated stress levels, suggesting that this percentage is optimal for maximising elastic properties. Typically, materials with enhanced RM values can better distribute stresses within the pavement structure, thereby contributing to a potential reduction in layer thickness [66,67] and resulting in overall cost savings.

Any deviation from the 3 % of cement content results in a corresponding variation in the RM values. Mixtures containing 2 % of cement exhibit slightly lower RM values, indicating a reduction in stiffness compared to those with 3 % of cement content. Moreover, the mixtures with 4 % of cement have the lowest stiffness among the investigated compositions. This is due to the shrinkage-induced cracking phenomena that occur during the curing stage, which are reflected in a reduction of RM values, consistent with previous studies [68–70]. However, the relatively low RM values obtained for the CDW+2%CEM-II/B mixtures

Table 3
Life cycle inventory of 1 Mg of CEM-II/B and CEM-IV/B.

Flow	Quantity		Unit of measure	Note
	CEM-II/B	CEM-IV/B		
Outputs				
Cement powder	1.0	1.0	Mg	
Particulate matter	1.2	1.2	g	
Inputs				
Fuel	1.07	1.07	MJ	Diesel burned in building machines
Electricity MV	35	36	kWh	MV = Medium voltage
Heat	$3.1 \cdot 10^{-2}$	$2.7 \cdot 10^{-2}$	MJ	
Cement factory	$2.73 \cdot 10^{-8}$	$2.73 \cdot 10^{-8}$	Item	
Clinker	790–650 *	640–450 *	kg	Dataset modelled with primary data from the plant. The clinker inventory is not available for confidential reasons.
Limestone	350–210 *	0	kg	
Gypsum	35	35	kg	
Industrial pozzolana	0	550–360 *	kg	Mainly composed of fly ash and waste clay* *
Other raw materials (i.e., ferrous sulphate, organic additives)	0–50 *	0–50 *	kg	
Transport of materials	77.8	140	Mg·km	Cumulative transport of all materials included in the production of cement.

Additional note:
* ranges from EN 197–1, the exact values cannot be provided for confidential reasons.
* * waste clay is deemed to be derived from the production of expanded clay (secondary data retrieved from *Ecoinvent* database); economic allocation is used (expanded clay: 1 €/kg; calcinated clay 0.10 €/kg).

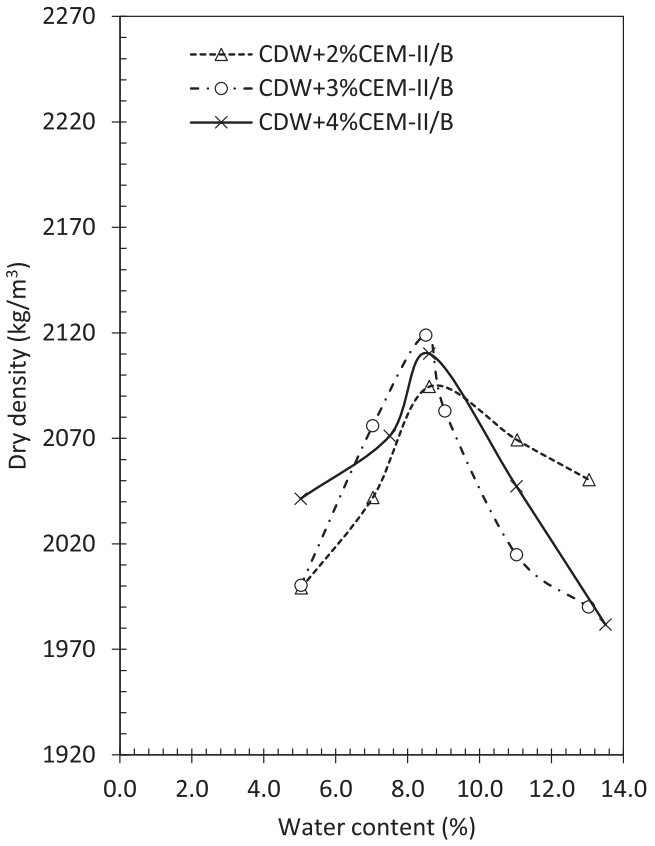


Fig. 3. Proctor compaction results for CDW-RA stabilised with 2, 3, and 4 % of CEM-II/B.

suggest that this quantity of cement was too low for the development of sufficiently strong bonds, at least in the case of short-term curing (i.e., 7 days).

Table 4
Mix-design and mixture designation.

Mixture designation	Aggregate	Binder	Binder dosage (%)
CDW+3%CEM-II/B	CDW-RA	CEM-II/B	3
CDW+3%CEM-IV/B	CDW-RA	CEM-IV/B	3
CDW+3%CEM-IV/H	CDW-RA	CEM-IV/H	3
CDW+8.5%AS	CDW-RA	AS	8.5

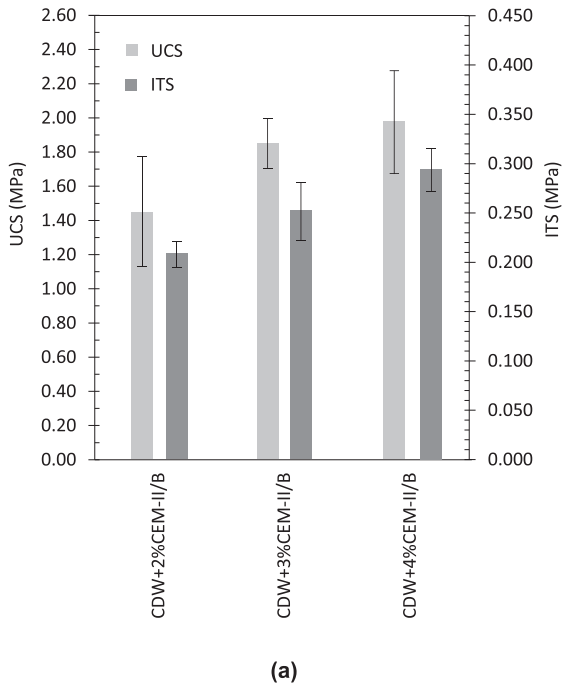
Table 4 provides a summary of the investigated stabilised mixtures. In part 2 of the experimental investigation, 3 % of cement was added to stabilise CDW-RA. Based on the Proctor and mechanical test results, this percentage (i) maximises the density of mixtures, (ii) leads to the highest RM value, and (iii) is the lowest value that meets the UCS and ITS limits of the Technical Specifications for road subbase layers [46,64,65].

The Proctor test showed that the optimum amount of alkaline solution required to stabilise CDW-RA was 8.5 % of the dry mass of the aggregates (Fig. 5).

4.2. Phase 2: comparison between different binder types

The compaction curves for CDW-RA mixtures stabilised with CEM-IV/B, CEM-IV/H, and AA-CDW fines are shown in Fig. 5. Both CDW+3%CEM-IV/B and CDW+3%CEM-IV/H mixtures required the same amount of w_{opt} (8.5 %) as the reference mixture (CDW+3%CEM-II/B) to achieve a maximum dry density of 2090 kg/m^3 (for CDW+3% CEM-IV/B) and 2088 kg/m^3 (for CDW+3%CEM-IV/H). The addition of 8.5 % in mass of dry CDW-RA of alkaline liquids resulted in a $\gamma_{d,max}$ of 2164 kg/m^3. It is important to note that the addition of the AS had the dual purpose of (i) providing workability to the mixture and (ii) triggering the AA of CDW-RA fines. In conclusion, an optimum liquid content of 8.5 % was used to stabilise the mixtures, regardless of the type of binder used (i.e., cement or AS).

The strength test results given in Fig. 6-a indicate that the addition of 3 % of CEM-IV/B instead of CEM-II/B had a negligible effect on the UCS and ITS values of the stabilised CDW-RA mixtures. In particular, the CDW+3%CEM-IV/B mixture achieved an average UCS of



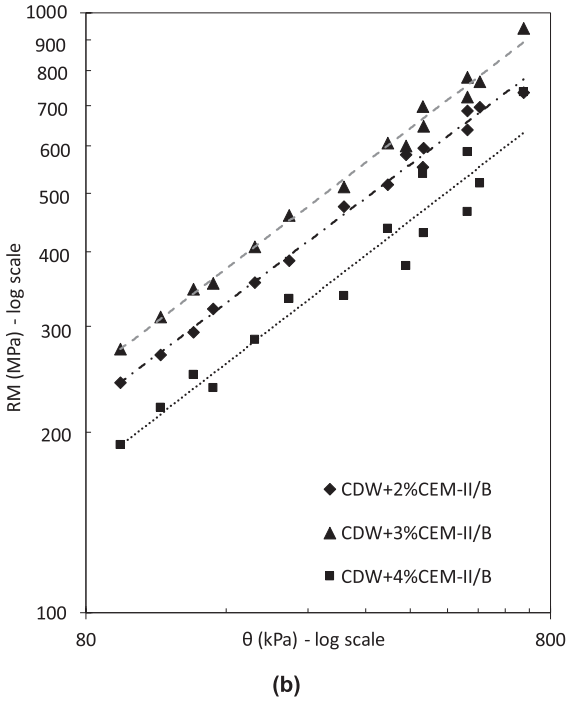


Fig. 4. Mechanical testing results for CDW-RA stabilised with different percentages of CEM-II/B. (a) Average values of UCS and ITS (error bars indicate one standard deviation). (b) RM results as a function of the first invariant (θ).

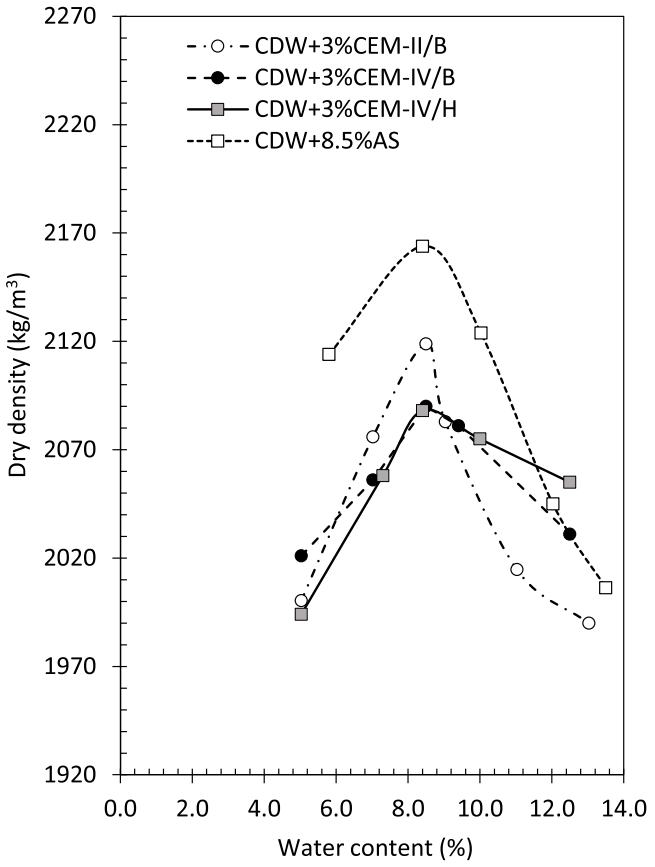


Fig. 5. Proctor compaction results for CDW-RA stabilised with AS, CEM-II/B, CEM-IV/B, and CEM-IV/H.

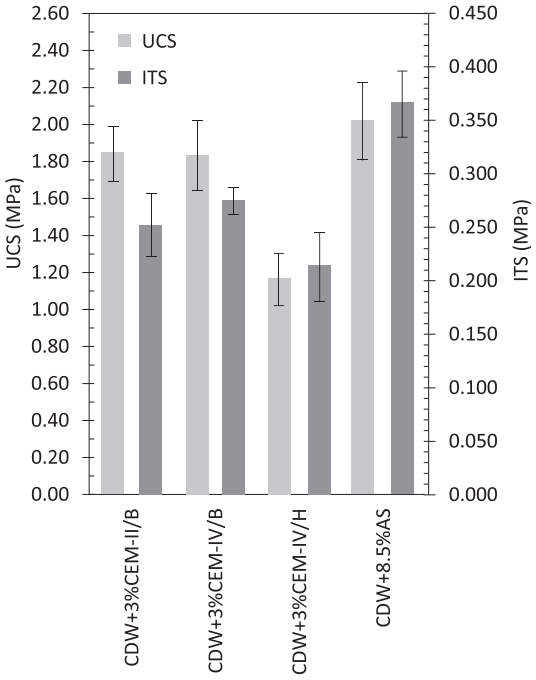
1.83 MPa and ITS of 0.276 MPa compared to the values of 1.85 MPa (UCS) and 0.252 MPa (ITS) obtained with the reference mixture (CDW+3%CEM-II/B). However, when CEM-IV/H was used as a binder to stabilise CDW-RA, a reduction of more than 50 % in UCS was observed in comparison to CDW+3%CEM-IV/B. It is worth noting that the CDW+3%CEM-V/H mixture did not achieve the minimum UCS value for the subbase/subgrade layer for flexible pavements [65] and the threshold of 0.250 MPa established in the Italian Technical Specifications [46] for ITS. It is reasonable to assume that the low clinker content in CEM-IV/H hindered pozzolanic reactions with the added WC, especially given the limited curing time of 7 days [71].

The AA of fine particles in CDW-RA mixtures resulted in the formation of a material with excellent strength properties. The CDW+8.5%AS samples achieved the highest UCS and ITS values among all stabilised mixtures, with an average value of 2.02 MPa and 0.367 MPa, respectively. This result meets the requirements of the M-EPDG [65] and confirms the superior performance of this alternative stabilisation technique [41].

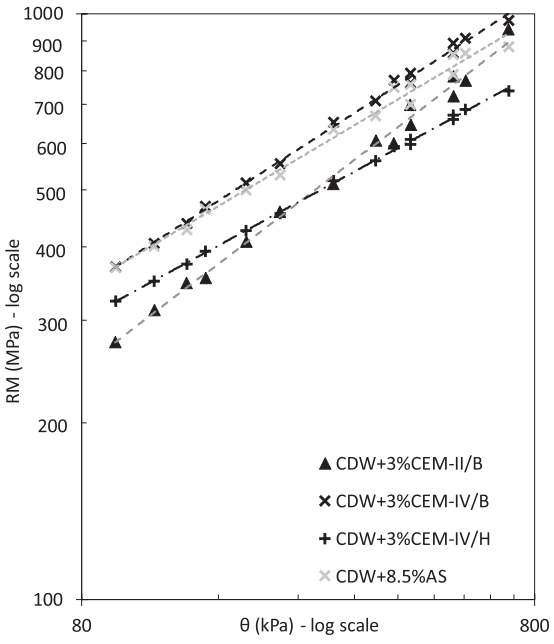
As shown in Fig. 6-b, the addition of 3 % of CEM-IV/B resulted in a significant increase in stiffness as evidenced by the highest RM values obtained over all the stress state ranges investigated. Similarly, the CDW+8.5%AS exhibited excellent resilient behaviour, with values on average 17 % higher than the reference mixture (CDW+2%CEM-II/B). The mixture containing the hybrid cement (CDW+3%CEM-IV/H) performed reasonably well compared to the reference (CDW+3%CEM-II/B). Specifically, at low-stress levels ($\theta < 200$ kPa), the RM of CDW+3% CEM-IV/H is slightly higher than the reference, while at higher stress levels, the CDW+3%CEM-IV/B mixture exhibits lower values.

4.3. *Life-cycle assessment*

The LCA inventory for stabilised mixtures containing the same CDW-RA but with different binder types is reported in Table 5. The LCA analysis results to produce 1 Mg of stabilised CDW-RA with 3 % wt. of



(a)



(b)

Fig. 6. Mechanical testing results for CDW-RA stabilised with 3 % CEM-II/B (reference), 3 % CEM-IV/B, 3 % CEM-IV/H, and 8.5 %f AS. (a) Average values of UCS and ITS (error bars indicate one standard deviation). (b) RM results as a function of the first invariant (θ).

Table 5
Life cycle inventory of 1 Mg of stabilised CDW-RA mixture for different binder types.

Flow	Quantity				Unit of measure	Note
	CDW+3% CEM-II/B	CDW+3%CEM-IV/B	CDW+3%CEM-IV/H	CDW+8.5% AS		
Outputs						
	1.03	1.03	1.03	1.085	Mg	
Inputs						
Electricity MV	0.082	0.082	0.082	0.082	kWh	MV = Medium voltage
CDW-RA	1.0	1.0	1.0	1.0	Mg	Reference to Table 2
CEM-II/B	30	0	0	0	kg	Reference to Table 3
CEM-IV/B	0	30	15	0	kg	Reference to Table 3
Waste clay (WC)	0	0	15	0	kg	
Alkaline solution (AS)	0	0	0	85	kg	Sodium silicate (Na_2SiO_3) derived from hydrothermal liquor process and deionised water (*Ecoinvent* database)
Water	85	85	85	0	kg	
Transport of materials	4.5	4.5	6.8	21.3	Mg·km	Cumulative transport of all materials included in the production of the stabilised CDW-RA mixture

Table 6
Impact results related to the production of 1 Mg of stabilised CDW-RA mixture depending on the binder.

Impact category	Unit	Mixture			
		CDW+ 3%CEM-II/B	**CDW+ 3%CEM-IV/B**	**CDW+ 3%CEM-IV/H**	**CDW+ 8.5%AS**
Acidification	mol H^+ eq.	3.26	2.18	1.10	2.09
Climate change	kg CO_2 eq.	24.1	19.9	14.3	42.2
Ecotoxicity, freshwater - inorganics	CTUe	15000	10000	5030	258
Particulate matter	disease inc.	$2.18{\cdot}10^{-5}$	$1.48{\cdot}10^{-5}$	$7.75{\cdot}10^{-6}$	$2.42{\cdot}10^{-6}$
Eutrophication, marine	kg N eq.	0.0665	0.0474	0.0273	0.0422
Eutrophication, freshwater	kg P eq.	0.0010	0.0014	0.0012	0.0151
Eutrophication, terrestrial	mol N eq.	7.65	5.11	2.60	4.36
Human toxicity, cancer	CTUh	$8.35{\cdot}10^{-4}$	$5.54{\cdot}10^{-4}$	$2.77{\cdot}10^{-4}$	$2.57{\cdot}10^{-8}$
Human toxicity, non-cancer	CTUh	$8.89{\cdot}10^{-2}$	$5.90{\cdot}10^{-2}$	$2.95{\cdot}10^{-2}$	$7.96{\cdot}10^{-7}$
Ionising radiation	kBq U_{235} eq.	0.402	0.376	0.303	4.060
Land use	Pt	63.2	65.6	66.9	224.0
Ozone depletion	kg CFC−11 eq.	$2.75{\cdot}10^{-7}$	$2.48{\cdot}10^{-7}$	$2.13{\cdot}10^{-7}$	$1.38{\cdot}10^{-5}$
Photochemical ozone formation	kg NMVOC eq.	32.80	21.80	10.90	0.15
Resource use, fossils	MJ	153.0	152.0	137.0	563.0
Resource use, minerals, and metals	kg Sb eq.	$4.15{\cdot}10^{-5}$	$3.99{\cdot}10^{-5}$	$4.05{\cdot}10^{-5}$	$5.72{\cdot}10^{-4}$
Water use	m^3 depriv.	5.10	4.90	4.56	27.8

Note:
- "mol H+ eq." represents the potential acidification of soils and water due to the release of nitrogen oxides and sulphur oxides [72];
- "CTUe" is the comparative toxic unit referred to as "ecotoxicity" and indicates the impact of toxic substances on freshwater organisms [73];
- "disease inc." is the disease incidence. It suggests the potential incidence of disease due to particulate matter emissions [59];
- "CTUh" is the comparative toxic unit referred to human health and indicates the impact on humans of toxic substances emitted to the environment, divided into non-cancer and cancer-related toxic substances [73];
- "kBq U_{235} eq." indicates the quantity in Bq (Becquerel) of ionising radiation on the population in comparison to Uranium 235 [73];
- "Pt" means points and it is a dimensionless measure and indicates the changes in soil quality [74];
- "kg CFC-11 eq." quantifies the ozone depletion potential of different gases relative to the reference substance chlorofluorocarbon-11 [75];
- "kg NMVOC eq." measures the emissions of non-methane volatile organic compounds (NMVOC) that can lead to the creation of photochemical smog [76];
- "kg Sb eq." is the equivalent of kilograms of antimony which contributes to resource depletion [59];
- "m3 depriv." indicates the relative amount of water used [59].

different types of cement (CEM-II/B, CEM-IV/B, and CEM-IV/H) and 8.5 % of AS are shown in Table 6. Among the aggregates stabilised with cement, the CDW+3%CEM-II/B mixture has the highest impact on most of the indicators (except for freshwater eutrophication, land use and minerals and metals resource use), followed by CDW+3%CEM-IV/B and CDW+3%CEM-IV/H. With regard to the climate change indicator, the CDW+3%CEM-IV/H mixture was found to have the lowest impact. However, it should be noted that this material had inferior mechanical properties compared to the others (Section 4).

The CDW+8.5%AS mixture has a relatively low environmental impact for eight of the sixteen indicators studied, namely acidification, freshwater ecotoxicity, particulate matter, marine eutrophication, terrestrial eutrophication, cancer and non-cancer human toxicity, and photochemical ozone formation. Conversely, the same mixture shows the highest value for the climate change indicator (42.2 kg CO_2 eq.), which raises concerns about its environmental impact.

5. Discussion

5.1. Mechanical performance

Fig. 7 presents a correlation between the mean values of UCS (Fig. 7-a) and ITS (Fig. 7-b) and the mean bulk density of the specimens (Section 3.1). It is worth noting that the gyratory compaction process resulted in densities that were 5–6 % higher than the Proctor values. During gyratory compaction, the material undergoes a kneading action generated by the combination of vertical pressure and internal shear stresses. The 1.25° inclined rotation around the vertical axis induces internal stresses which facilitate movement between grains, thereby improving the compaction attitude [77,78]. Furthermore, both Fig. 7-a and Fig. 7-b indicate that the stabilised mixtures with the highest UCS and ITS values also exhibited slightly higher densities. It can therefore be suggested that, in addition to the effects of binder properties, the measured

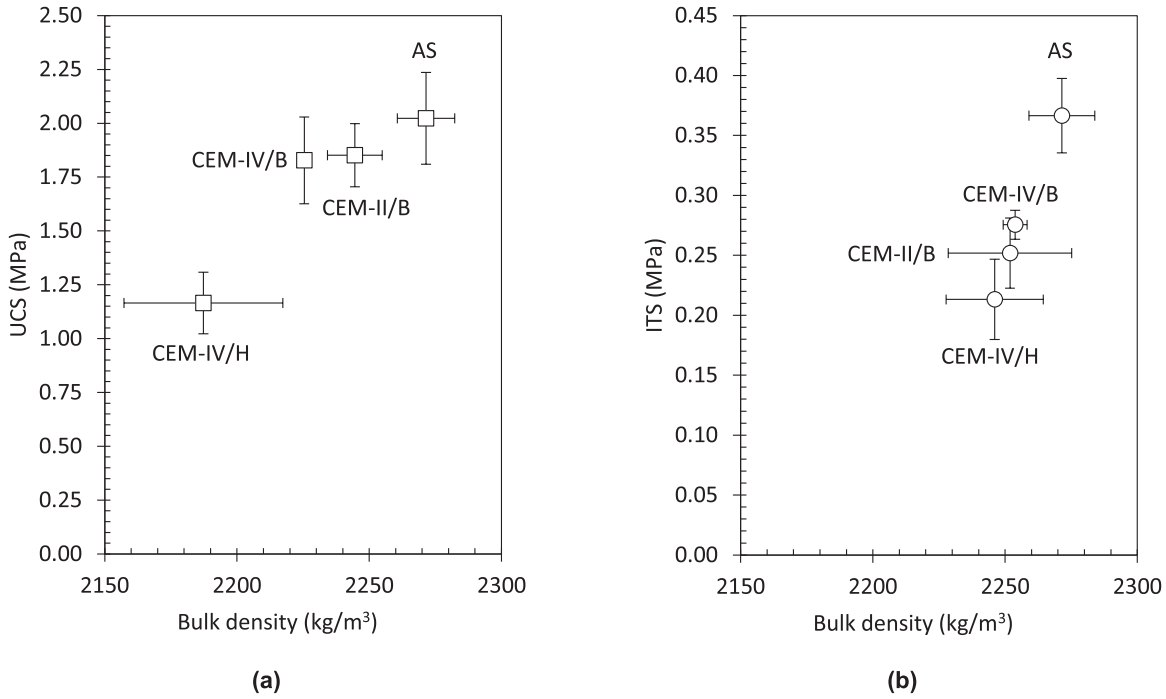


Fig. 7. Average (a) UCS and (b) ITS results as a function of the bulk density of specimens.

strength and stiffness may have been influenced by the density of the material.

An examination of the three different types of cement, all added to the CDW-RA mixture with the same 3 % wt., reveals that the pozzolanic cement CEM-IV/B demonstrates comparable strength properties to those of CDW+3%CEM-II/B. The independent sample *t*-test showed no significant differences in UCS and ITS values between the CDW+3%CEM-II/B and CDW+3%CEM-IV/B mixtures (both *p*-values > 0.05). In terms of stiffness, Table 7 summarises the regression parameters k_1, k_2, and k_3 obtained by fitting the M-EPDG model (Eq. 1) to the RM results. Considering only the mixtures containing cement, the CDW+3%CEM-IV/B material outperforms all the others, with a k_1 value (proportional to the material Young's modulus) that is significantly higher than that for the CDW+3%CEM-II/B mixture. When examining the k_2 parameter, both CDW-RA mixtures stabilised with CEM-IV and CEM-II show similar behaviour, indicating their stress-hardening characteristics. The k_3 parameter of CDW+3%CEM-IV/B shows a negative value (−0.144), indicating that an increase in shear deformation likely due to an increase in octahedral shear stress leads to a reduction in elastic properties.

The excellent mechanical properties of the CDW+3%CEM-IV/B mixture (−1 % UCS, +9 % ITS, and an average +22 % RM compared to the reference mixture) suggest that the IP in CEM-IV/B was highly effective in inducing pozzolanic reactions in the mixture. It is reasonable to assume that the pozzolana reacts with the calcium hydroxide from the clinker hydration to form additional calcium-silicate-hydrated (C-S-H) products which strengthen the matrix [79,80]. In other words, the equivalent strength properties of CEM-II/B and CEM-IV/B cements suggest that the lower clinker content in CEM-IV/B is effectively compensated for by the pozzolanic activity of the added IP. The initial strength development is initiated by the available clinker, and the subsequent pozzolanic reactions continue to provide excellent strength and stiffness to the stabilised CDW-RA mixture.

Conversely, the experimental low-clinker cement derived from the combination of CEM-IV/B and WC used to stabilise CDW-RA gives a lower level of mechanical performance than the other two types of cement (CEM-II/B and CEM-IV/B), particularly in the UCS test. The clinker content in the CEM-IV/H may be insufficient to effectively initiate the pozzolanic reactions of the added WC, especially given the limited curing time of 7 days. The excessive concentration of inactive minerals and the presence of pores in the binding matrix limited the formation of calcium-hydrated species and the strength development [81,82]. In addition, the reduction in reaction kinetics due to the addition of WC, often observed in previous studies [83], hindered strength development. Nevertheless, the elastic properties of the CDW-RA stabilised with 3 % of CEM-IV/H align with those of the reference mixture. The regression parameters in Table 7 indicate that the CDW+3%CEM-IV/H mixture has (i) a k_1 value which is slightly higher than that of the reference mixture, (ii) a stress-hardening behaviour in line with all the other mixtures ($k_2 > 0$), and (iii) a k_3 parameter close to zero ($k_3 = -0.068$), indicating the reduced influence of the octahedral stress on the resilient behaviour.

According to the mechanical test results, Portland-limestone and pozzolanic cements are effective in stabilising CDW-RA. However, the low clinker content prevents full activation of the waste pozzolana, resulting in a deterioration of the mechanical properties, which can be compensated by increasing the amount of binder.

The addition of alkaline liquids for CDW-RA stabilisation produced a mixture with mechanical performance superior to that of the mixture produced with CEM-II/B. In terms of UCS (Fig. 7-a), the CDW+8.5%AS mixture achieved values comparable to those of the CDW-RA stabilised

Table 7
Regression parameters and model fitting evaluation of RM test results by the M-EPDG.

Material	M-EPDG model parameters			Statistics of the model fitting	
	k_1	k_2	k_3	R^2	Se/Sy*
CDW+3%CEM-II/B	2739	0.514	0.275	0.91	0.31
CDW+3%CEM-IV/B	3824	0.538	−0.144	0.88	0.36
CDW+3%CEM-IV/H	3297	0.439	−0.068	0.95	0.23
CDW+8.5%AS	3868	0.536	−0.280	0.88	0.36

Notes:
*Se/Sy represents the standard error of estimate (Se) over the standard deviation (Sy). The magnitude of this ratio indicates the goodness-of-fit as "excellent" for Se/Sy ≤ 0.35, "good" for 0.36 ≤ Se/Sy ≤ 0.55, "fair" for 0.56 ≤ Se/Sy ≤ 0.75, and "poor" for 0.76 ≤ Se/Sy ≤ 0.90 [88]

with 4 % CEM-II/B, while the same mixture exhibited the highest ITS values (Fig. 7-b). Similarly, the fitting of the RM results (Eq. 1) from the CDW+8.5%AS mixture shows the highest k_1 parameter, indicating excellent elastic behaviour. However, the k_3 parameter of −0.280 suggests that increases in deviatoric stress led to significant reductions in RM values.

The evolution of strength and stiffness in CDW-RA mixtures containing AS suggests the formation of soluble silica species resulting in a highly crystalline AA structure. The presence of sodium silicate contributes to a robust interface, thereby enhancing the overall mechanical strength. Given the highly crystalline nature of CDW fines and the relatively low curing temperature (i.e., at room temperature rather than the 60–80°C thermal treatment typically used to activate alkaline reactions of aluminosilicates), the development of mechanical properties is likely to result from both the sodium silicate solidification and the alkaline activation of the finest grains [41].

This was confirmed by microscopic analysis, which reveals the formation of a well-developed crystalline structure and a dense matrix structure [28,84,85]. In contrast to similar studies ([86,87]), in which CDW-RA was stabilised by the addition of highly AA-reactive precursors (i.e. FA and BFS), the stabilisation in the CDW+8.5%AS material is carried out without the addition of any external materials, i.e., neither cement nor reactive AA precursors.

5.2. Environmental performance

Fig. 8 provides a graphical representation of the LCA outcomes for the investigated mixtures in relative terms, where the higher value is set as 100 % for each indicator. When comparing the three cement-stabilised mixtures, i.e., CDW+3%CEM-II/B, CDW+3%CEM-IV/B, and CDW+3%CEM-IV/H, a reduction in the cement clinker content reduces the impact for most of the indicators. This is mainly due to the direct emissions generated during the calcination process in the production of clinker [89–91]. For this reason, the mixture with CEM-IV/B is more sustainable than the mixture with CEM-II/B. Similarly, since CEM-IV/H has half the clinker content of CEM-IV/B, the CDW+3%CEM-IV/H mixture has the lowest environmental impact albeit its mechanical performance is also lower. In line with previous studies [92,93], the transport of materials over long distances (more than 100 km) has a relevant environmental impact, an example being the transport of fly ash used for IP production (Fig. 9-a).

Fig. 10 shows the main contributors to each environmental indicator related to the production of the CDW+3%CEM-IV/B mixture. Considering the total climate change impact indicator (equal to 19.9 kg CO_2 eq. per Mg of stabilised mixture), 65 % is due to CEM-IV/B, added at a rate of 3 % in the mass of dry aggregates. For this cement, the main contribution (55 % of the overall impact) is due to the clinker, mainly because of the high temperature and direct emissions generated during its production. In contrast, the addition of IP contributed 7 % to the total climate change, while the transport of materials to the cement plant contributed 6 %. In general, the addition of just 3 % of cement is responsible for most of the impacts associated with the production of cement-stabilised CDW-RA. This is also a crucial consideration in the selection of the binder addition percentage within the mixture. Focusing only on the climate change indicator, an LCA simulation was conducted where the cement content in CEM-II/B, CEM-IV/B, and CEM-IV/H was varied between 2 % and 4 %. A variation of ± 1 % (one percentage point) in the cement content resulted in variations of ± 24, ± 23, and ± 22 % in the impact figures for the CDW-RA mixture with CEM-II/B, CEM-IV/B, and CEM-IV/H respectively. A reduction in the quantity of cement added is advisable to reduce the environmental impact associated with the stabilisation of recycled CDW-RA with conventional Portland-limestone cement.

In addition to cement, the contribution of the CDW-RA in the stabilised mixture should not be disregarded for climate change, freshwater eutrophication, ionising radiation, land use, ozone depletion, fossil/

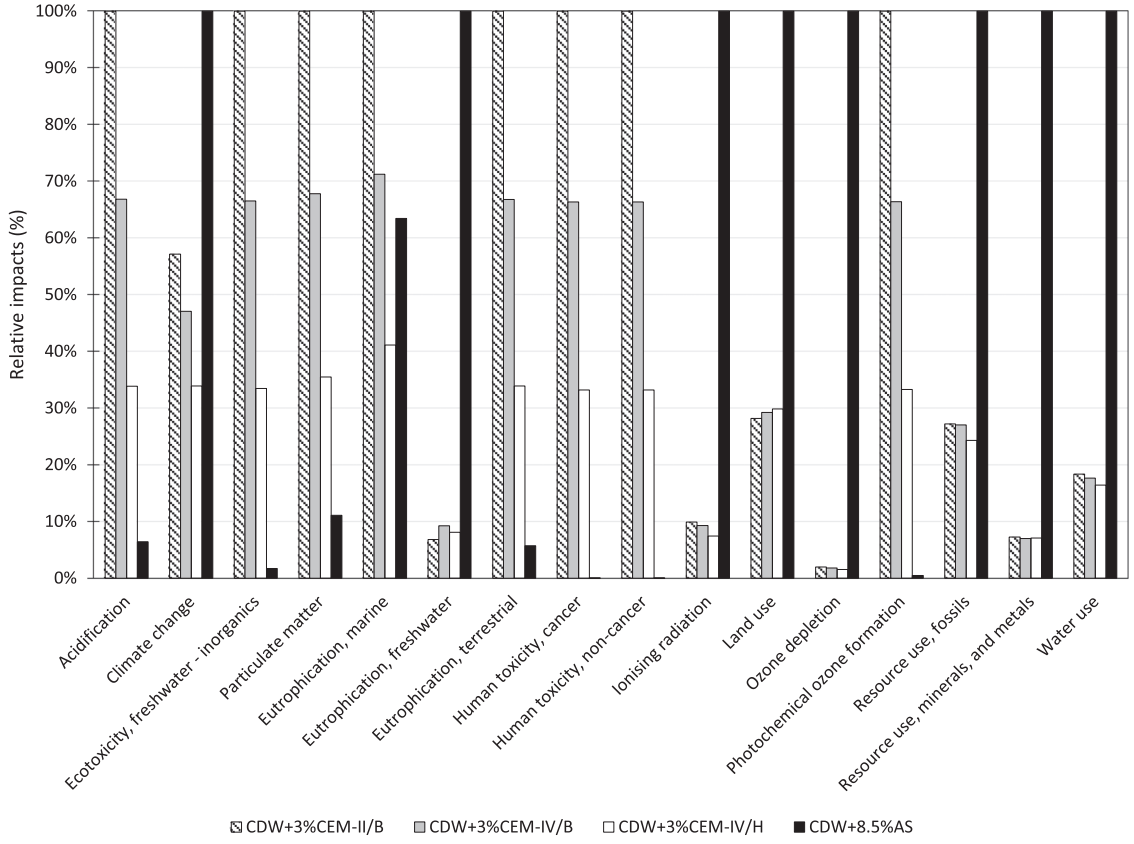


Fig. 8. Relative environmental impact associated with the production of 1 Mg of stabilised CDW-RA mixture depending on the binder.

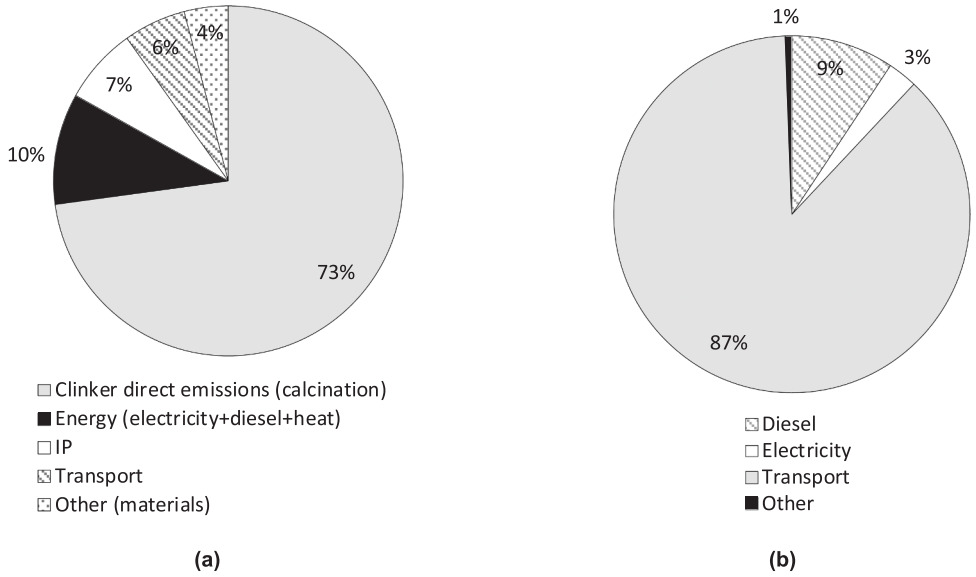


Fig. 9. Contribution analysis for the climate change indicator of (a) CEM-IV/B and (b) the CDW-RA.

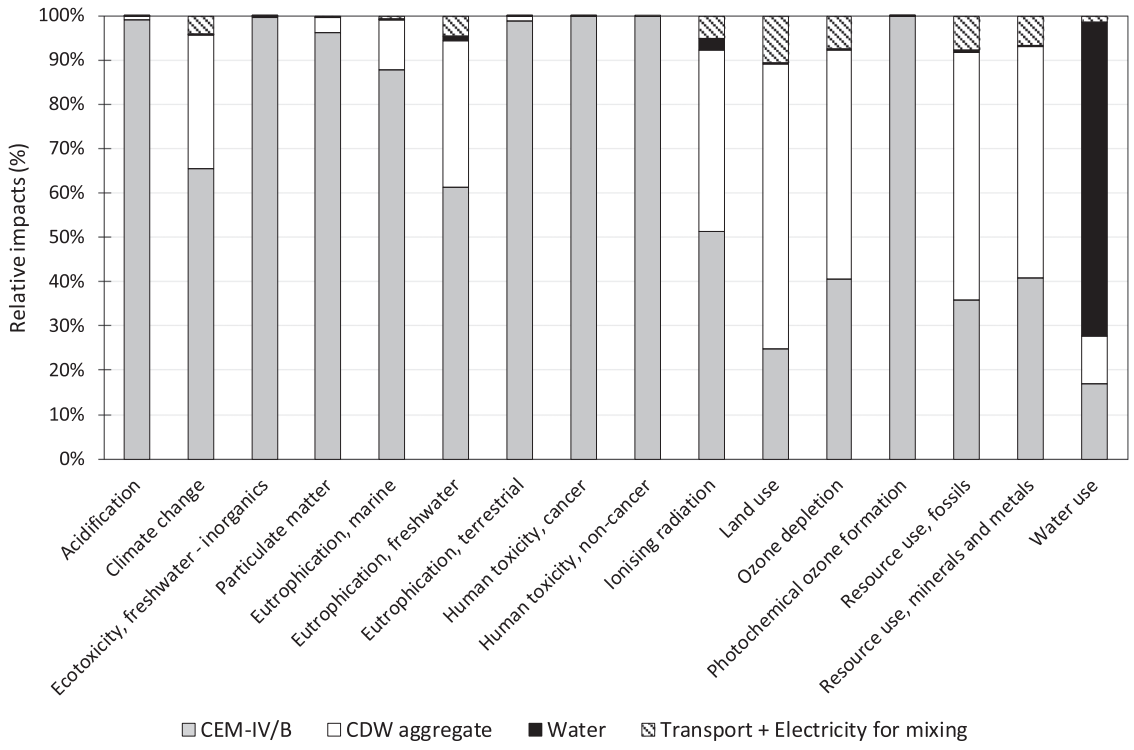


Fig. 10. Contribution analysis of the stabilised aggregates with 3 % CEM IV/B.

minerals, and metals resource use indicators. For these indicators, the main contribution of CDW-RA is associated with road transport as shown in Fig. 9-b.

The environmental impacts associated with CDW+8.5%AS are not entirely favourable, especially when compared to CDW-RA stabilised with cementitious products. In detail, the LCA results show a lower impact for eight out of sixteen indicators, but for other categories, the environmental performance is not as favourable as it could be. The high value for climate change (42.2 kg CO_2 eq./Mg) is mainly due to the production of sodium silicate used in the AS (78 %). AS is also the main contributor to all the other impact indicators (Fig. 11), a finding that is consistent with previous analyses [94,95]. The remaining part of the total impact is due to the transport of materials to the production plant and to the process by which CDW is treated to obtain RA. In this LCA study, a dataset from the *Ecoinvent* database was used to approximate the production of sodium silicate in Europe compared to the hydrothermal liquor process [61]. This source shows that the impact of sodium silicate is mainly due to the high amount of electricity required for the production.

Alkaline activation offers several advantages in terms of bearing capacity and resistance to traffic loads because of their superior mechanical properties. However, it requires further optimisation to mitigate some environmental impacts. The results indicate that the mixture CDW+8.5%AS can be more sustainable and cheaper by (i) improving

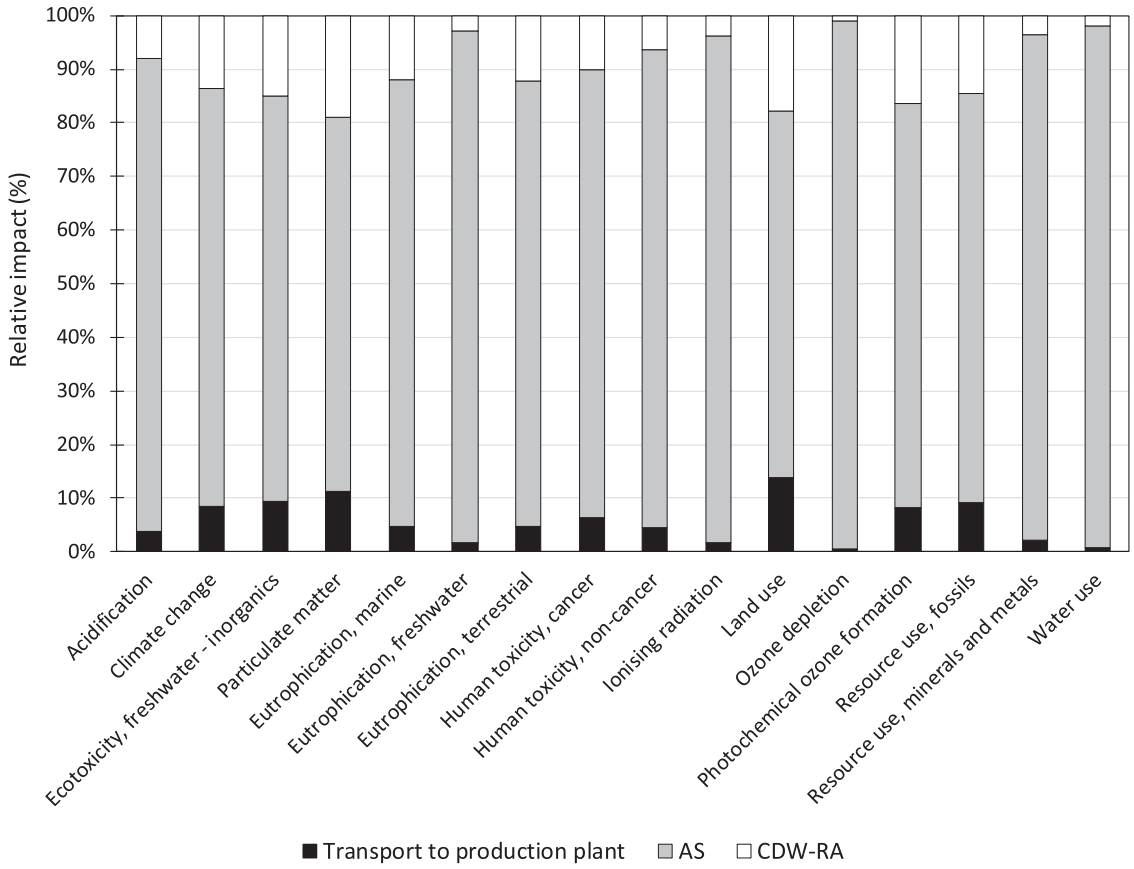


Fig. 11. Contribution analysis of the stabilised aggregates with 8.5 % AS.

the wettability of the viscous solution, (ii) reducing the energy required to produce the AS (e.g., by using renewable energy and waste raw materials), and (iii) reducing the transport distances from production to mixing plants.

6. Conclusion

This study investigated the mechanical and environmental performance of CDW-RA mixtures stabilised with cementitious and alkali-activated (AA) binders. It aimed to provide a comprehensive understanding of the performance and sustainability of such stabilisation techniques.

The following conclusions were drawn:

- the properties of stabilised CDW-RA mixtures were significantly influenced by the type and quantity of binders used, with all binders having noticeable effects on mixture strength, stiffness, and environmental impact;
- the addition of 3 % of Portland-limestone and pozzolanic cement to stabilise CDW-RA results from a trade-off between maximising structural properties (UCS, ITS, RM) and limiting environmental impact;
- the LCA analysis highlighted the crucial role of the cement content in the environmental impact of stabilised RA mixtures; an incremental addition of 1 % in cement results in a 24 % and 23 % increase of climate change impact, for Portland-limestone and pozzolanic cement, respectively;
- while pozzolanic cement does not produce significant changes in strength (UCS and ITS) compared to Portland-limestone cement, it does produce significant increases in stiffness (RM), resulting in the improved structural response of the pavement; as a result, the reduced amount of clinker used serves to reduce the environmental impact (e.g., −18 % climate change) compared to Portland-limestone cement;
- the addition of waste pozzolana to pozzolanic cement (CEM-IV/H) minimises the presence of clinker in the stabilised RA mixture, with significant environmental benefits (−41 % and −28 % climate change than mixtures with Portland-limestone and pozzolanic cement, respectively), but with a deterioration in mechanical properties of around −37 % in UCS and −15 % in the ITS compared to Portland-limestone cement;
- due to its viscous nature, which affects the wettability of the aggregate, alkaline solutions must be added in larger quantities (8.5 % by mass of aggregate) to obtain a mechanical performance superior to that of the CDW-RA mixture stabilised with Portland-limestone cement (+9 % for UCS, 46 % for ITS, +17 % for RM);
- the environmental impact of AS exhibits both favourable (−94 % acidification, −98 % freshwater ecotoxicity, −89 % particulate matter, −37 % marine eutrophication, −94 % terrestrial eutrophication) and unfavourable (+75 % in climate change, +255 % in land use) outcomes compared to traditional CDW-RA mixtures stabilised with Portland-limestone cement; this increased impact is due to the energy-intensive production process of alkaline liquids and the distances involved in their transport;
- the current limitations of stabilisation technology with AS can be overcome by (i) reducing its viscosity to improve the aggregate wettability, (ii) decreasing the energy required for production and, (iii) reducing transport distances through a wider availability.

Using these results as a starting point, a more comprehensive analysis can be carried out to assess the environmental impact of the entire pavement structure. In this way, it would be possible to determine the effect of different stabilised CDW granular materials on the structural and environmental performance of road pavements. This approach

would enable decision-makers and practitioners to select the most appropriate material and construction process required to optimise both the field performance and environmental sustainability of these materials.

CRediT authorship contribution statement

Bianco Isabella: Writing – original draft, Validation, Software, Methodology, Investigation, Data curation. **Bassani Marco:** Writing – review & editing, Supervision, Resources, Methodology, Funding acquisition, Conceptualization. **Tefa Luca:** Writing – review & editing, Writing – original draft, Supervision, Methodology, Investigation, Funding acquisition, Formal analysis, Data curation.

Declaration of Competing Interest

The authors declare that they have no known competing financial interests or personal relationships that could have appeared to influence the work reported in this paper.

Acknowledgements

The research was funded with the European Regional Development Fund by the Regione Piemonte (P.O.R. FESR 2014-2020, Asse I, Azione I.1b.1.2, PRISM-E) in the frame of INTREC project (INnovative Technologies for RECycled aggregates from construction and demolition waste in road constructions, request code 337-303) in cooperation with CAVIT S.p.A.

Data availability

Data will be made available on request.

References

[1] P. Ghisellini, M. Ripa, S. Ulgiati, Exploring environmental and economic costs and benefits of a circular economy approach to the construction and demolition sector. A literature review, J. Clean. Prod. 178 (2018) 618–643, https://doi.org/10.1016/j.jclepro.2017.11.207.
[2] L.A. López Ruiz, X. Roca Ramón, S. Gassó Domingo, The circular economy in the construction and demolition waste sector – a review and an integrative model approach, J. Clean. Prod. 248 (2020) 119238, https://doi.org/10.1016/j.jclepro.2019.119238.
[3] K. Nunes, C. Mahler, Comparison of construction and demolition waste management between Brazil, European Union and USA, Waste Manag Res 38 (2020) 415–422, https://doi.org/10.1177/0734242X20902814.
[4] Y. Zhao, D. Goulias, L. Tefa, M. Bassani, Life cycle economic and environmental impacts of CDW recycled aggregates in roadway construction and rehabilitation, Sustainability 13 (2021) 8611, https://doi.org/10.3390/su13158611.
[5] R. Cardoso, R.V. Silva, J. de Brito, R. Dhir, Use of recycled aggregates from construction and demolition waste in geotechnical applications: a literature review, Waste Manag. 49 (2016) 131–145, https://doi.org/10.1016/j.wasman.2015.12.021.
[6] Z. Abedin Khan, U. Balunaini, S. Costa, N.H.T. Nguyen, A review on sustainable use of recycled construction and demolition waste aggregates in pavement base and subbase layers, Clean. Mater. 13 (2024) 100266, https://doi.org/10.1016/j.clema.2024.100266.
[7] G. Tavakoli Mehrjardi, A. Azizi, A. Haji-Azizi, G. Asdollafardi, Evaluating and improving the construction and demolition waste technical properties to use in road construction, Transp. Geotech. 23 (2020) 100349, https://doi.org/10.1016/j.trgeo.2020.100349.
[8] J. Zhang, L. Ding, F. Li, J. Peng, Recycled aggregates from construction and demolition wastes as alternative filling materials for highway subgrades in China, J. Clean. Prod. 255 (2020) 120223, https://doi.org/10.1016/j.jclepro.2020.120223.
[9] J. Zhang, F. Gu, Y. Zhang, Use of building-related construction and demolition wastes in highway embankment: laboratory and field evaluations, J. Clean. Prod. 230 (2019) 1051–1060, https://doi.org/10.1016/j.jclepro.2019.05.182.
[10] I. Del Rey, J. Ayuso, A. Barbudo, A.P. Galvín, F. Agrela, J. de Brito, Feasibility study of cement-treated 0–8 mm recycled aggregates from construction and demolition waste as road base layer, Road. Mater. Pavement Des. 17 (2016) 678–692, https://doi.org/10.1080/14680629.2015.1108221.
[11] P. Pérez, F. Agrela, R. Herrador, J. Ordoñez, Application of cement-treated recycled materials in the construction of a section of road in Malaga, Spain, Constr. Build. Mater. 44 (2013) 593–599, https://doi.org/10.1016/j.conbuildmat.2013.02.034.
[12] E. Garzón, S. Martínez-Martínez, L. Pérez-Villarrejo, P.J. Sánchez-Soto, Assessment of construction and demolition wastes (CDWs) as raw materials for the manufacture of low-strength concrete and bases and sub-bases of roads, Mater. Lett. 320 (2022) 132343, https://doi.org/10.1016/j.matlet.2022.132343.
[13] I.A. Beja, R. Motta, L.B. Bernucci, Application of recycled aggregates from construction and demolition waste with Portland cement and hydrated lime as pavement subbase in Brazil, Constr. Build. Mater. 258 (2020) 119520, https://doi.org/10.1016/j.conbuildmat.2020.119520.
[14] Md.U. Hossain, C.S. Poon, Y.H. Dong, D. Xuan, Evaluation of environmental impact distribution methods for supplementary cementitious materials, Renew. Sustain. Energy Rev. 82 (2018) 597–608, https://doi.org/10.1016/j.rser.2017.09.048.
[15] J. Skibsted, R. Snellings, Reactivity of supplementary cementitious materials (SCMs) in cement blends, Cem. Concr. Res. 124 (2019) 105799, https://doi.org/10.1016/j.cemconres.2019.105799.
[16] M.C.G. Juenger, R. Snellings, S.A. Bernal, Supplementary cementitious materials: new sources, characterization, and performance insights, Cem. Concr. Res. 122 (2019) 257–273, https://doi.org/10.1016/j.cemconres.2019.05.008.
[17] J.S.J. van Deventer, J.L. Provis, P. Duxson, D.G. Brice, Chemical research and climate change as drivers in the commercial adoption of alkali activated materials, Waste Biomass Valoriz. 1 (2010) 145–155, https://doi.org/10.1007/s12649-010-9015-9.
[18] B.C. McLellan, R.P. Williams, J. Lay, A. van Riessen, G.D. Corder, Costs and carbon emissions for geopolymer pastes in comparison to ordinary portland cement, J. Clean. Prod. 19 (2011) 1080–1090, https://doi.org/10.1016/j.jclepro.2011.02.010.
[19] S.H. Teh, T. Wiedmann, A. Castel, J. de Burgh, Hybrid life cycle assessment of greenhouse gas emissions from cement, concrete and geopolymer concrete in Australia, J. Clean. Prod. 152 (2017) 312–320, https://doi.org/10.1016/j.jclepro.2017.03.122.
[20] E.D. Rodríguez, S.A. Bernal, J.L. Provis, J. Paya, J.M. Monzo, M.V. Borrachero, Effect of nanosilica-based activators on the performance of an alkali-activated fly ash binder, Cem. Concr. Compos. 35 (2013) 1–11, https://doi.org/10.1016/j.cemconcomp.2012.08.025.
[21] D.A. Salas, A.D. Ramirez, N. Ulloa, H. Baykara, A.J. Boero, Life cycle assessment of geopolymer concrete, Constr. Build. Mater. 190 (2018) 170–177, https://doi.org/10.1016/j.conbuildmat.2018.09.123.
[22] P. Duxson, J.L. Provis, Designing precursors for geopolymer cements, J. Am. Ceram. Soc. 91 (2008) 3864–3869, https://doi.org/10.1111/j.1551-2916.2008.02787.x.
[23] F. Pacheco-Torgal, J. Castro-Gomes, S. Jalali, Alkali-activated binders: a review. Part 2. About materials and binders manufacture, Constr. Build. Mater. 22 (2008) 1315–1322, https://doi.org/10.1016/j.conbuildmat.2007.03.019.
[24] D.M. González-García, L. Téllez-Jurado, F.J. Jiménez-Álvarez, H. Balmori-Ramírez, Structural study of geopolymers obtained from alkali-activated natural pozzolan feldspars, Ceram. Int. 43 (2017) 2606–2613, https://doi.org/10.1016/j.ceramint.2016.11.070.
[25] M. Najimi, N. Ghafoori, M. Sharbaf, Alkali-activated natural pozzolan/slag mortars: a parametric study, Constr. Build. Mater. 164 (2018) 625–643, https://doi.org/10.1016/j.conbuildmat.2017.12.222.
[26] N. Cristelo, J. Coelho, T. Miranda, Á. Palomo, A. Fernández-Jiménez, Alkali activated composites – an innovative concept using iron and steel slag as both precursor and aggregate, Cem. Concr. Compos. 103 (2019) 11–21, https://doi.org/10.1016/j.cemconcomp.2019.04.024.
[27] J. Van De Sande, A. Peys, T. Hertel, H. Rahier, Y. Pontikes, Upcycling of non-ferrous metallurgy slags: identifying the most reactive slag for inorganic polymer construction materials, Resour. Conserv. Recycl. 154 (2020) 104627, https://doi.org/10.1016/j.resconrec.2019.104627.
[28] L. Tefa, M. Bassani, B. Coppola, P. Palmero, Strength development and environmental assessment of alkali-activated construction and demolition waste fines as stabilizer for recycled road materials, Constr. Build. Mater. 289 (2021) 123017, https://doi.org/10.1016/j.conbuildmat.2021.123017.
[29] C. Ferone, F. Colangelo, F. Messina, L. Santoro, R. Cioffi, Recycling of pre-washed municipal solid waste incinerator fly ash in the manufacturing of low temperature setting geopolymer materials, Materials 6 (2013) 3420–3437, https://doi.org/10.3390/ma6083420.
[30] N. Cristelo, L. Segadães, J. Coelho, B. Chaves, N.R. Sousa, M. de Lurdes Lopes, Recycling municipal solid waste incineration slag and fly ash as precursors in low-range alkaline cements, Waste Manag. 104 (2020) 60–73, https://doi.org/10.1016/j.wasman.2020.01.013.
[31] L. Tefa, I. Bianco, G.A. Blengini, M. Bassani, Integrated and comparative Structural-LCA analysis of unbound and cement-stabilized construction and demolition waste aggregate for subbase road pavement layers formation, J. Clean. Prod. 352 (2022) 131599, https://doi.org/10.1016/j.jclepro.2022.131599.
[32] A. Mohammadinia, A. Arulrajah, J. Sanjayan, M.M. Disfani, M. Win Bo, S. Darmawan, Stabilization of demolition materials for pavement base/subbase applications using fly ash and slag geopolymers: laboratory investigation, J. Mater. Civ. Eng. 28 (2016) 04016033, https://doi.org/10.1061/(ASCE)MT.1943-5533.0001526.
[33] A. Arulrajah, A. Mohammadinia, A. D'Amico, S. Horpibulsuk, Cement kiln dust and fly ash blends as an alternative binder for the stabilization of demolition aggregates, Constr. Build. Mater. 145 (2017) 218–225, https://doi.org/10.1016/j.conbuildmat.2017.04.007.
[34] T. Poltue, A. Suddeepong, S. Horpibulsuk, W. Samingthong, A. Arulrajah, A.S. A. Rashid, Strength development of recycled concrete aggregate stabilized with fly ash-rice husk ash based geopolymer as pavement base material, Road. Mater.

Pavement Des. 21 (2020) 2344–2355, https://doi.org/10.1080/14680629.2019.1593884.
[35] T. Manohar, N.V. Rao, J.P. Giri, in: A.K. Agnihotri, K.R. Reddy, H.S. Chore (Eds.), Utilization of Different Supplementary Cementitious Materials and Recycled Concrete Aggregate for Stabilization of Pavement Base Layer, Proceedings of Indian Geotechnical and Geoenvironmental Engineering Conference (IGGEC) 2021, Vol. 2, Springer Nature, Singapore, 2023, pp. 139–146, https://doi.org/10.1007/978-981-19-4731-5_12.
[36] N. Yadav, R. Kumar, B. Jethy, Influence of supplementary cementitious materials along with construction and demolition waste in pavement cement-treated subbase applications, Innov. Infrastruct. Solut. 9 (2024) 65, https://doi.org/10.1007/s41062-023-01358-5.
[37] M. Bassani, L. Tefa, B. Coppola, P. Palmero, Alkali-activation of aggregate fines from construction and demolition waste: valorisation in view of road pavement subbase applications, J. Clean. Prod. 234 (2019) 71–84, https://doi.org/10.1016/j.jclepro.2019.06.207.
[38] European Committee for Standardization, Cement - Part 1: Composition, specifications and conformity criteria for common cements, (2011).
[39] M. Kristmann, Portland cement clinker: Mineralogical and chemical investigations: Part I Microscopy, X-ray fluorescence and X-ray diffraction, Cem. Concr. Res. 7 (1977) 649–658, https://doi.org/10.1016/0008-8846(77)90047-3.
[40] S. Khelifi, F. Ayari, H. Tiss, D.B. Hassan Chehimi, X-ray fluorescence analysis of Portland cement and clinker for major and trace elements: accuracy and precision, J. Aust. Ceram. Soc. 53 (2017) 743–749, https://doi.org/10.1007/s41779-017-0087-x.
[41] M. Bassani, L. Tefa, A. Russo, P. Palmero, Alkali-activation of recycled construction and demolition waste aggregate with no added binder, Constr. Build. Mater. 205 (2019) 398–413, https://doi.org/10.1016/j.conbuildmat.2019.02.031.
[42] European Committee for Standardization, Tests for general properties of aggregates - Part 1: Methods for sampling, (1996).
[43] European Committee for Standardization, Tests for geometrical properties of aggregates - Part 11: Classification test for the constituents of coarse recycled aggregate, (2009).
[44] M. Bassani, L. Tefa, Compaction and freeze-thaw degradation assessment of recycled aggregates from unseparated construction and demolition waste, Constr. Build. Mater. 160 (2018) 180–195, https://doi.org/10.1016/j.conbuildmat.2017.11.052.
[45] A. Barbudo, F. Agrela, J. Ayuso, J.R. Jiménez, C.S. Poon, Statistical analysis of recycled aggregates derived from different sources for sub-base applications, Constr. Build. Mater. 28 (2012) 129–138, https://doi.org/10.1016/j.conbuildmat.2011.07.035.
[46] Centro Sperimentale Interuniversitario di Ricerca Stradale, Studio a carattere pre-normativo delle norme tecniche di tipo prestazionale per capitolati speciali d'appalto, (2001).
[47] European Committee for Standardization, Tests for mechanical and physical properties of aggregates - Part 6: Determination of particle density and water absorption, (2013).
[48] European Committee for Standardization, Tests for geometrical properties of aggregates - Part 3: Determination of particle shape - Flakiness index, (2012).
[49] European Committee for Standardization, Tests for geometrical properties of aggregates - Part 4: Determination of particle shape - Shape index, (2008).
[50] European Committee for Standardization, Unbound and hydraulically bound mixtures - Part 2: Test methods for laboratory reference density and water content - Proctor compaction, (2010).
[51] American Association of State and Highway Transportation Officials, Standard method of test for determining the resilient modulus of soils and aggregate materials, (2013).
[52] American Association of State Highway and Transportation Officials, Mechanistic-empirical pavement design guide: a manual of practice, 2015.
[53] R. Ji, N. Siddiki, T. Nantung, D. Kim, Evaluation of resilient modulus of subgrade and base materials in indiana and its implementation in MEPDG, Sci. World J. 2014 (2014) 372838, https://doi.org/10.1155/2014/372838.
[54] S.M.R.M. Chowdhury, E. Kassem, Estimation of resilient modulus constitutive model parameters for unbound coarse materials for MEPDG, J. Transp. Eng., Part B: Pavements 148 (2022) 04022040, https://doi.org/10.1061/JPEODX.0000378.
[55] M. Bassani, P.P. Riviera, L. Tefa, G. Chiappinelli, Effects of quantity and plasticity of fine particles on the workability and resilient behaviour of aggregate-soil mixtures for granular pavement layers, Road. Mater. Pavement Des. 22 (2021) 444–463, https://doi.org/10.1080/14680629.2019.1633390.
[56] International Organization for Standardization, Environmental management - Life cycle assessment - Principles and framework, 2006.
[57] International Organization for Standardization, Environmental management - Life cycle assessment - Requirements and guidelines, 2006.
[58] European Commission - Joint Research Centre - Institute for Environment and Sustainability, International Reference Life Cycle Data System (ILCD) Handbook - General guide for Life Cycle Assessment - Provisions and Action Steps, Publications Office of the European Union, Luxembourg, 2010.
[59] European Commission, Commission recommendation of 16.12.2021 on the use of the Environmental Footprint methods to measure and communicate the life cycle environmental performance of products and organisations, 2021. ⟨https://environment.ec.europa.eu/publications/recommendation-use-environmental-footprint-methods_en⟩.
[60] Y.H. Huang. Pavement Analysis and Design, second ed., Pearson, Upper Saddle River, NJ, 2003.
[61] G. Wernet, C. Bauer, B. Steubing, J. Reinhard, E. Moreno-Ruiz, B. Weidema, The ecoinvent database version 3 (part I): overview and methodology, Int J. Life Cycle Assess. 21 (2016) 1218–1230, https://doi.org/10.1007/s11367-016-1087-8.
[62] S. Fazio, L. Zampori, A. De Schryver, O. Kusche, L. Thellier, E. Diaconu, Guide for EF compliant data sets, Version 2.0. Joint Research Center, Luxembourg, European Commission, 2020.
[63] Cavit S.P.A., Environmental Declaration, Turin, Italy, 2022.
[64] Department of the Army, Department of the Air Force, Pavement design for roads, streets, and open storage areas, elastic layered method, Washington, D.C., 1994.
[65] Applied Research Associates Inc., Guide for Mechanistic-Empirical Design of New and Rehabilitated Pavement Structures, Transportation Research Board, National Research Council, Washington, D.C., 2004.
[66] J. Song, W.Y. Cui, Y.Y. Fan, The influence analysis of the soil base and the base stiffness of highway asphalt pavement on pavement thickness, Appl. Mech. Mater. 178–181 (2012) 1406–1409, https://doi.org/10.4028/www.scientific.net/AMM.178-181.1406.
[67] N. Su, F. Xiao, J. Wang, S. Amirkhanian, Characterizations of base and subbase layers for mechanistic-empirical pavement design, Constr. Build. Mater. 152 (2017) 731–745, https://doi.org/10.1016/j.conbuildmat.2017.07.060.
[68] M. Bassani, P.P. Riviera, L. Tefa, Short-term and long-term effects of cement kiln dust stabilization of construction and demolition waste, J. Mater. Civ. Eng. 29 (2016) 04016286, https://doi.org/10.1061/(ASCE)MT.1943-5533.0001797.
[69] Z. Guotang, S. Wei, Y. Guotao, P. Li, C. Degou, J. Jinyang, H. Hao, Mechanism of cement on the performance of cement stabilized aggregate for high speed railway roadbed, Constr. Build. Mater. 144 (2017) 347–356, https://doi.org/10.1016/j.conbuildmat.2017.03.194.
[70] W. Li, L. Lang, Z. Lin, Z. Wang, F. Zhang, Characteristics of dry shrinkage and temperature shrinkage of cement-stabilized steel slag, Constr. Build. Mater. 134 (2017) 540–548, https://doi.org/10.1016/j.conbuildmat.2016.12.214.
[71] M. Ben Haha, P. Termkhajornkit, A. Ouzia, S. Uppalapati, B. Huet, Low clinker systems - Towards a rational use of SCMs for optimal performance, Cem. Concr. Res. 174 (2023) 107312, https://doi.org/10.1016/j.cemconres.2023.107312.
[72] M. Margni, T. Gloria, J. Bare, J. Seppälä, B. Steen, J. Struijs, L. Toffoletto, O. Jolliet, Guidance on how to move from current practice to recommended practice in Life Cycle Impact Assessment, (2008).
[73] M. Damiani, N. Ferrara, F. Ardente, Understanding Product Environmental Footprint and Organisation Environmental Footprint methods, Joint Research Centre (European Commission), Brussels, Belgium, 2022. ⟨https://data.europa.eu/doi/10.2760/11564⟩ (accessed August 12, 2024).
[74] V. De Laurentiis, M. Secchi, U. Bos, R. Horn, A. Laurent, S. Sala, Soil quality index: Exploring options for a comprehensive assessment of land use impacts in LCA, J. Clean. Prod. 215 (2019) 63–74, https://doi.org/10.1016/j.jclepro.2018.12.238.
[75] E. Jacob-Lopes, L.Q. Zepka, M.C. Deprá, Chapter 3 - Methods of evaluation of the environmental impact on the life cycle, in: E. Jacob-Lopes, L.Q. Zepka, M.C. Deprá (Eds.), Sustainability Metrics and Indicators of Environmental Impact, Elsevier, 2021, pp. 29–70, https://doi.org/10.1016/B978-0-12-823411-2.00003-7.
[76] N.V. von der Assen, A.M.L. Lafuente, M. Peters, A. Bardow, Environmental Assessment of CO2 Capture and Utilisation, in: P. Styring, E.A. Quadrelli, K. Armstrong (Eds.), Carbon Dioxide Utilisation, Elsevier, Amsterdam, 2015, pp. 45–56, https://doi.org/10.1016/B978-0-444-62746-9.00004-9.
[77] A.R. Dawson, Pavements Unbound, Proceedings of the 6th International Symposium on Pavement Unbound, 6-8 July, Nottingham, UK, Taylor & Francis Group, London, UK, 2004.
[78] G. Cerni, S. Camilli, Comparative analysis of gyratory and proctor compaction processes of unbound granular materials, Road. Mater. Pavement Des. 12 (2011) 397–421, https://doi.org/10.3166/rmpd.12.397-421.
[79] V.H. Dodson, Pozzolans and the Pozzolanic Reaction. in: Concrete Admixtures, Springer US, Boston, MA, 1990, pp. 159–201, https://doi.org/10.1007/978-1-4757-4843-7_7.
[80] A. Ahmed, Chemical reactions in pozzolanic concrete, MAMS 1 (2019), https://doi.org/10.32474/MAMS.2019.01.000120.
[81] J.M. Marangu, J.W. Muthengia, J.K. wa-Thiong'o, Performance of potential pozzolanic cement in chloride media, IOSR J. Appl. Chem. 7 (2014) 36–44.
[82] A. Tironi, C.C. Castellano, V.L. Bonavetti, M.A. Trezza, A.N. Scian, E.F. Irassar, Kaolinitic calcined clays – Portland cement system: hydration and properties, Constr. Build. Mater. 64 (2014) 215–221, https://doi.org/10.1016/j.conbuildmat.2014.04.065.
[83] A.A. Amer, S. El-Hoseny, Properties and performance of metakaolin pozzolanic cement pastes, J. Therm. Anal. Calor. 129 (2017) 33–44, https://doi.org/10.1007/s10973-017-6087-9.
[84] M.A. Villaquirán-Caicedo, R. Mejía de Gutiérrez, Comparison of different activators for alkaline activation of construction and demolition wastes, Constr. Build. Mater. 281 (2021) 122599, https://doi.org/10.1016/j.conbuildmat.2021.122599.
[85] G. Yıldırım, A. Kul, E. Özçelikci, M. Şahmaran, A. Aldemir, D. Figueira, A. Ashour, Development of alkali-activated binders from recycled mixed masonry-originated waste, J. Build. Eng. 33 (2021) 101690, https://doi.org/10.1016/j.jobe.2020.101690.
[86] N. Cristelo, A. Fernández-Jiménez, C. Vieira, T. Miranda, Á. Palomo, Stabilisation of construction and demolition waste with a high fines content using alkali activated fly ash, Constr. Build. Mater. 170 (2018) 26–39, https://doi.org/10.1016/j.conbuildmat.2018.03.057.
[87] A. Arulrajah, A. Mohammadinia, I. Phummiphan, S. Horpibulsuk, W. Samingthong, Stabilization of recycled demolition aggregates by geopolymers comprising calcium carbide residue, fly ash and slag precursors, Constr. Build. Mater. 114 (2016) 864–873, https://doi.org/10.1016/j.conbuildmat.2016.03.150.

[88] T. Pellinen, M. Witczak, Use of stiffness of hot-mix asphalt as a simple performance test, Transp. Res. Rec.: J. Transp. Res. Board (2002) 80–90.
[89] L. Barcelo, J. Kline, G. Walenta, E. Gartner, Cement and carbon emissions, Mater. Struct. 47 (2014) 1055–1065, https://doi.org/10.1617/s11527-013-0114-5.
[90] J. Ke, M. McNeil, L. Price, N.Z. Khanna, N. Zhou, Estimation of CO2 emissions from China's cement production: methodologies and uncertainties, Energy Policy 57 (2013) 172–181, https://doi.org/10.1016/j.enpol.2013.01.028.
[91] N. Mohamad, K. Muthusamy, R. Embong, A. Kusbiantoro, M.H. Hashim, Environmental impact of cement production and solutions: a review, Mater. Today.: Proc. 48 (2022) 741–746, https://doi.org/10.1016/j.matpr.2021.02.212.
[92] Y. Li, Y. Liu, X. Gong, Z. Nie, S. Cui, Z. Wang, W. Chen, Environmental impact analysis of blast furnace slag applied to ordinary Portland cement production, J. Clean. Prod. 120 (2016) 221–230, https://doi.org/10.1016/j.jclepro.2015.12.071.
[93] D. Yang, L. Fan, F. Shi, Q. Liu, Y. Wang, Comparative study of cement manufacturing with different strength grades using the coupled LCA and partial LCC methods—a case study in China, Resour., Conserv. Recycl. 119 (2017) 60–68, https://doi.org/10.1016/j.resconrec.2016.06.017.
[94] M. Abdulkareem, J. Havukainen, J. Nuortila-Jokinen, M. Horttanainen, Environmental and economic perspective of waste-derived activators on alkali-activated mortars, J. Clean. Prod. 280 (2021) 124651, https://doi.org/10.1016/j.jclepro.2020.124651.
[95] K.K. Ramagiri, A. Kar, Environmental impact assessment of alkali-activated mortar with waste precursors and activators, J. Build. Eng. 44 (2021) 103391, https://doi.org/10.1016/j.jobe.2021.103391.